Infrared block of Na+ and Ca2+ spikes in in crayfish neuromuscular junction

Xuedong Zhu, Jen-Wei Lin, Michelle Y. Sander

Xuedong Zhu, Jen-Wei Lin, Michelle Y. Sander, "Infrared block of Na+ and Ca2+ spikes in in crayfish neuromuscular junction," Proc. SPIE 10866, Optogenetics and Optical Manipulation 2019, 108660E (22 February 2019); doi: 10.1117/12.2508996

SPIE.

Event: SPIE BiOS, 2019, San Francisco, California, United States

Infrared Block of Na^+ and Ca^{2+} Spikes in Crayfish Neuromuscular Junction

Xuedong Zhu[a], Jen-Wei Lin[b], Michelle Y. Sander[c,d,*]
[a]Department of Biomedical Engineering, Boston University, 44 Cummington Mall, Boston, MA 02215, USA
[b]Department of Biology, Boston University, 5 Cummington Mall, Boston, MA 02215, USA
[c]Department of Electrical and Computer Engineering and Boston University Photonics Center, Boston University, Boston, MA 02215, USA
[d]Division of Materials Science and Engineering, Boston University, Brookline, MA 02446, USA

ABSTRACT

Pulsed infrared (IR) light in the 1.8 - 2 μm region can modulate neural activities with high spatial and temporal precision. However, the mechanisms underlying these photothermal interactions are not fully understood. Here we investigate the IR modulation of axon and muscle activities using the crayfish (*Procambarus clarkii*) opener neuromuscular preparation. A modulated fiber coupled laser diode ($\lambda = 2$ μm) is used to deliver pulsed light with durations between 10 – 500 ms. Two-electrode current clamp (TECC) is performed to stimulate and monitor the neural activities. Laser-induced temperature changes are measured by an open patch pipette simultaneously with TECC. We find that IR pulses can reversibly inhibit or block axon (Na^+) and muscle (Ca^{2+}) spikes. In axons, single IR pulses can suppress the action potential (AP) amplitude and duration and increase the interspike interval. In addition, the rates of AP depolarization and repolarization are also modulated by IR pulses. Individual IR pulses can also block muscle fiber Ca^{2+} spikes. The IR-induced decrease in the input resistance (8.4%) can be a contributing factor for the inhibition phenomena reported here.

Keywords: infrared inhibition, neurons, muscle fibers, neural modulation, photothermal effect

INTRODUCTION

Control of neural and muscular activity is essential for both fundamental research and clinical applications. As an emerging novel technique, it has been demonstrated that interaction with infrared (IR) light can elicit nerve and muscle responses[1,2]. Such infrared nerve stimulation can have many advantages since it is contactless and damage-free, spatially precise and features minimal invasiveness over traditional electrical methods of neural stimulation. When IR light was applied to different neurons or cells to investigate the possible neural stimulation mechanisms, it has been found that the thermal transient induced by water absorption of IR can lead to neural activation[3]. Alterations of the membrane electrical capacitance caused by such transient heating has been demonstrated to depolarize cells and elicit action potentials (APs)[4,5]. IR light has also been shown to induce intracellular calcium modulations in neonatal ventricular cardiomycytes[6], in astrocytes and neurons in *vivo*[7], and in spiral and vestibular ganglion neurons[8]. Other postulated mechanisms associated with IR stimulation include the activation of temperature sensitive ion channels[9], the formation of nanopores in the plasma membrane[10], and optoacoustic effects[11, 12].

In addition to IR neural stimulation, suppression of neural activities and blocking of action potentials by pulsed IR light have been reported more recently in different tissue types, both in *vivo* and in *vitro*[13-18]. Reversible IR inhibition of embryonic hearts has also been presented[19]. Though it is largely understood that IR inhibition and stimulation both work through photothermal effects, the detailed dynamics of all the underlying biophysical mechanisms still remain largely unclear. One possible explanation is that temperature rise induced by IR pulses can change the membrane resistance and ion channel kinetics such that the neural activity is inhibited[18, 20, 21].

In this work, we study the mechanisms of IR inhibition of neural activities using the unmyelinated axons of the crayfish opener neuromuscular junction. We focus on evaluating the changes in input resistance and action potentials associated with pulsed IR light illumination through a fairly focused light delivery with a 50 μm diameter fiber core. High resolution

*msander@bu.edu; phone 617-358-0505; fax 617-353-7337; http://sites.bu.edu/ufolab/

Optogenetics and Optical Manipulation 2019, edited by Samarendra K. Mohanty, E. Duco Jansen, Proc. of SPIE Vol. 10866, 108660E · © 2019 SPIE · CCC code: 1605-7422/19/$18 · doi: 10.1117/12.2508996

electrophysiology recordings with microelectrodes is pursued: TECC is performed in order to reliably induce and measure neural and muscular activities. Single IR square pulses of different durations are delivered to the axon and muscle fiber. IR induced temperature changes are monitored with an open patch pipette simultaneously with electrophysiological recordings.

METHODS

2.1 Preparation and Electrophysiological Recording

Crayfish (*Procambarus clarkii*) of both sexes were purchased from Niles Biological Supplies (Sacramento, CA). The opener neuromuscular preparation from the first walking leg was dissected in saline containing (mM): 195 NaCl, 5.4 KCl, 13.5 $CaCl_2$, 2.6 $MgCl_2$, 10 HEPES (pH 7.4). Only the inhibitory motor axon (~ 30 µm in diameter) and muscle fibers were used for the recording. The saline was circulated by a peristaltic pump (Gilson Minipuls 2, Middleton, WI, USA) at a rate of 1.5 ml/min. In order to obtain consistent and stable AP firing, 4-aminopyridine (4-AP) at 200 µM was used in most preparations (recordings were started only after at least 20 minutes to ensure steady levels of blockage). The IR inhibition effects on AP firing were similar with and without 4-AP. All chemicals were purchased from Sigma-Aldrich.

Two-electrode current clamp (TECC) was performed with AXOCLAMP-2A (Axon Instruments Inc., CA, USA) and IE201 (Warner Instrument Corp., CT, USA). Voltage signals were filtered at 5 kHz and sampled at 50 kHz (NI USB 6361). Microelectrodes with 40 – 60 MΩ resistance were filled with 500 mM KCl for axonal recording. For muscular recording, microelectrode tips were beveled to 10 – 20 MΩ resistance and filled with 3 M KCl. For alignment and positioning the preparation was placed under an upright microscope with an Olympus 60X water immersion lens.

For the electrophysiology recording, two axonal electrodes were placed near the primary branch in a distal-to-proximal direction. The open patch pipette for temperature monitoring and optical fiber were positioned to approach the preparation from opposite directions (Fig. 1). The four elements were arranged at an angle around ~ 28° to the horizontal sample plane. For an optimized alignment, the optical fiber was first lowered to touch the surface of the cells before being lifted up slightly afterwards. A red laser diode was coupled to the optical fiber to visualize the invisible infrared laser illumination so that the current injection electrode could be located within close proximity of the illumination spot. The tip of the patch pipette was positioned around the center of the illuminated area near the current injection electrode. Axon penetration and placement of the optical fiber and patch electrode were performed under the 60X water immersion lens.

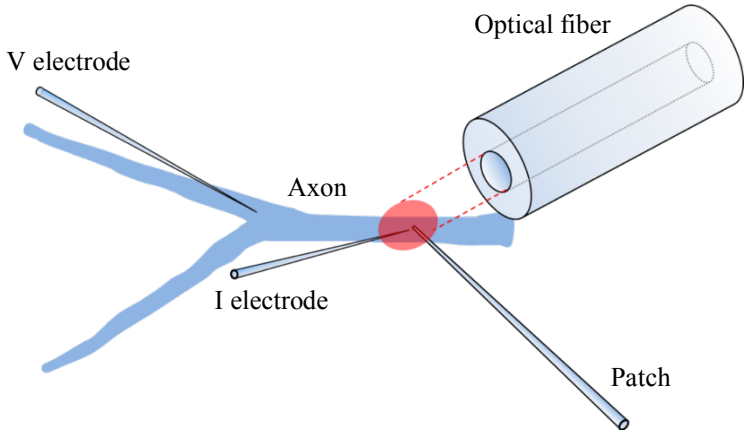

Figure 1: Schematic configuration of the experiment on the crayfish opener neuromuscular preparation. The current injection electrode (I electrode) to elicit APs is located closer to the primary branch of the inhibitory axon and the voltage recording electrode (V electrode) is placed ~ 200 µm to 300 µm from the branching point. An optical fiber with a 50 µm core diameter tilted at an angle of ~ 28° to the horizontal sample plane delivers the pulsed infrared light. The tip of an open patch pipette is placed close to the axon and I electrode.

2.2 Infrared Light Exposure

A fiber-coupled diode laser (FPL2000S, Thorlabs, Inc.) with a wavelength centered around 2 µm was used as the illumination source for the infrared inhibition experiments. The delivery fiber pigtail with a core diameter of 50 µm was

cleaved every time before each experiment. Single IR square pulses with varying durations were used in this report. The output power values refer to measurements at the delivery end of the fiber pigtail focused on the crayfish preparation. The output power and duration of the IR square pulses were modulated by a data acquisition platform (NI USB 6221).

2.3 Temperature Recording

An open patch pipette with a resistance around ~ 5 MΩ and filled with saline was used to monitor temperature changes induced by the infrared light illumination[22]. The perfusion tubing for circulating saline was fixed to a Peltier coupled copper plate to heat or cool the saline entering the recording chamber. The bath temperature was monitored with a small thermometer (BAT-12, Physitemp Instruments). Voltage steps between +5 mV to +15 mV were applied to the patch pipette. The natural logarithm applied to the Arrhenius equation (Eq. (1)) was used to estimate the activation energy (E_a) of the saline. In the following equation,

$$\ln(I) = \frac{E_a}{R}\frac{1}{T_0} + \ln(I_0) - \frac{E_a}{R}\frac{1}{T} \tag{1}$$

T is the saline temperature in Kelvin, I is the step voltage clamp current at corresponding temperature, T_0 is the room temperature, I_0 is the current step recorded at T_0, and R is gas constant. Fig. 2A illustrates the corresponding Arrhenius plot with $\ln(I)$ plotted on the y-axis versus $1/T$ measured between 283.2 K to 316.2 K on the x-axis. The averaged E_a for the extracellular saline solution was 3.7 ± 0.08 kcal mol^{-1} (mean $\pm$ standard error of mean (SEM), evaluated over 5 experiments ($N = 5$)) and was used to calculate the IR induced temperature transient according to Eq. (2). Representative temperature transients for a single pulse are shown in Figure 2B. The IR power in this experiment was kept constant at 7.1 mW with durations varying from 1 ms up to 500 ms. The associated temperature rise varied between 2 ℃ (1 ms) to 12℃ (500 ms) and it reached a plateau after ~ 200 ms and then decayed exponentially, as expected.

$$T = \frac{1}{\frac{1}{T_0} - \frac{R}{E_a}\ln\left(\frac{I}{I_0}\right)} \tag{2}$$

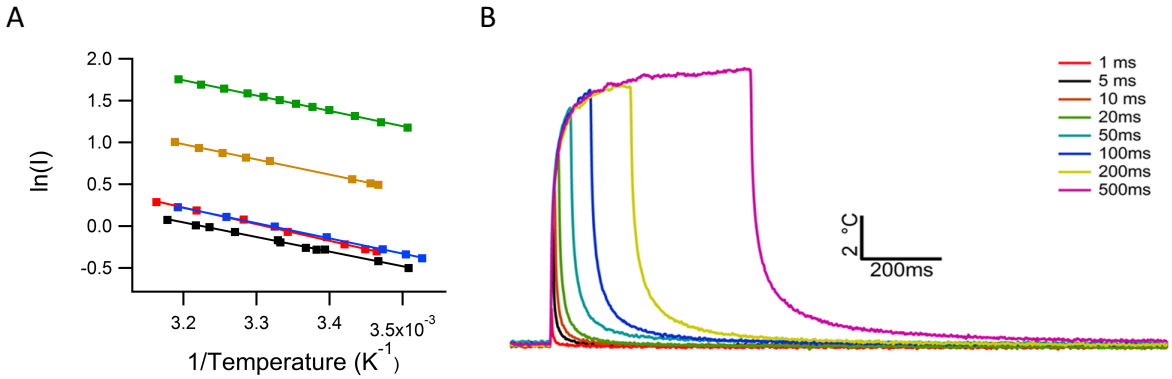

Figure 2: Calibration of E_a and examples of recorded temperature transients. (A) Arrhenius plot for determining the activation energy of the extracellular saline solution, $N = 5$. Different colors represent calibration sessions obtained from different pipettes. (B) Representative traces for the induced temperature transients of a single pulse with durations varying between 1 ms to 500 ms.

RESULTS

3.1 Short IR Pulse Suppresses AP Amplitude and Duration and Ca^{2+} Spike

The effect of short IR pulses (20 ms, 7.1 mW) on neural activities was first tested. AP trains activated by a current step of 22 nA were repeated with (red) and without (blue) illumination from a single IR pulse (Fig. 3A). A reduction in the amplitudes of two APs is observed. The temperature increase associated with such a single IR pulse was 8.7 ± 0.26 ℃ (mean $\pm$ SEM, $N = 5$), estimated by the open patch technique (see the green trace in Fig. 2B for example). The comparison of AP waveforms on an expanded time scale shows that both the AP amplitude and duration are reduced by the IR pulse

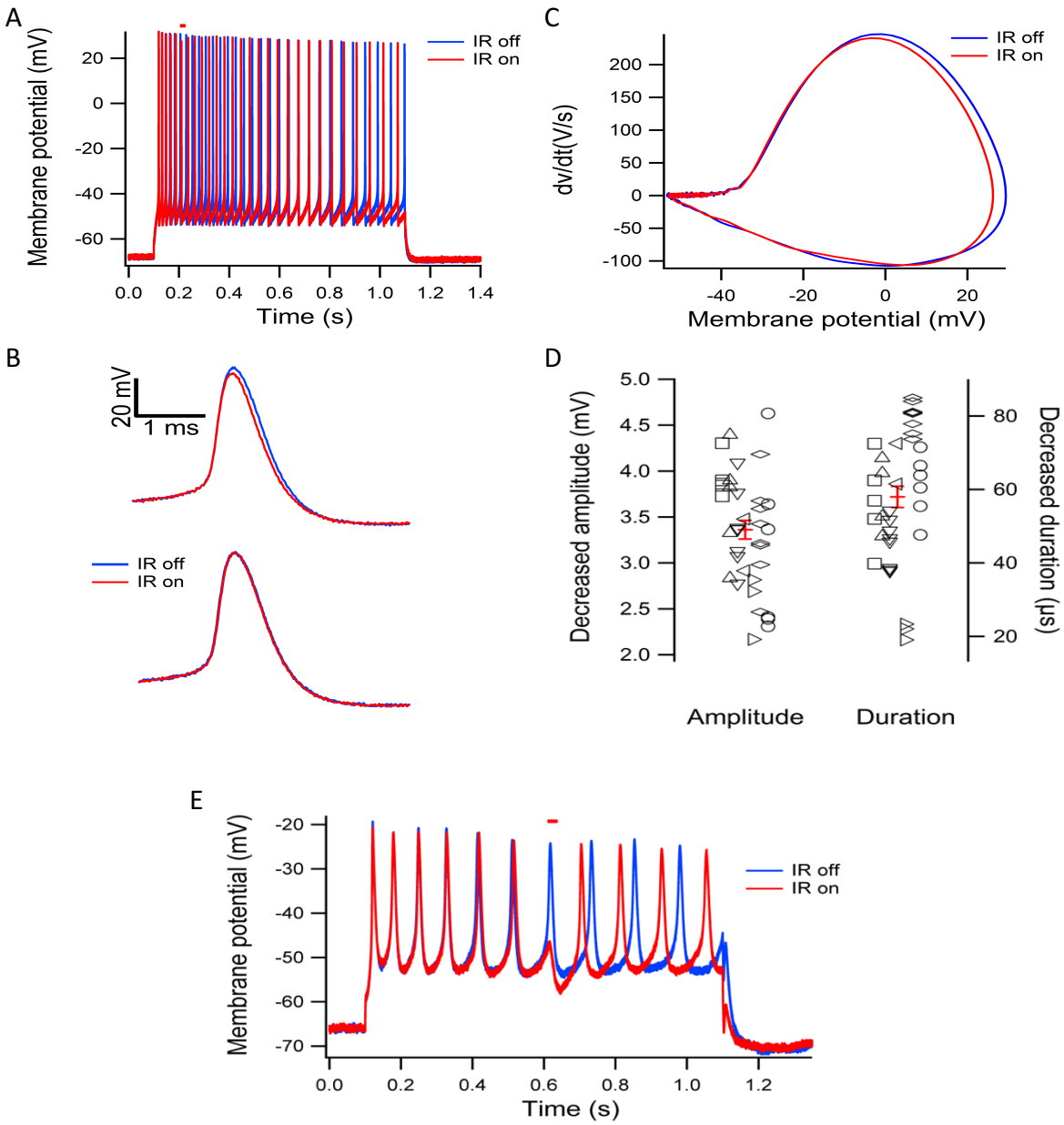

Figure 3: Impact of 20 ms IR pulses on the suppression of the AP amplitude and duration. (A) Representative traces with (red, IR on) and without (blue, IR off) a single pulse IR illumination. The red bar above the AP traces indicates the timing of IR pulse. (B) Comparison of AP waveforms with an expanded time scale during (top) and ~50 ms after (bottom) IR pulses. (C) Phase plots of two APs with and without IR pulse illumination. (D) The IR pulse reduces the AP amplitude and duration, analyzed here for $N = 7$. Each type of symbols represents data from one preparation. The average and standard error of the mean for decreased AP amplitude and duration are highlighted in red and amount to 3.4 ± 0.06 mV and 101 ± 2.9 µs. (E) IR inhibition of Ca^{2+} spike in crayfish muscle fiber. The red bar above the trace indicates the timing and duration of the single IR pulse.

(Fig. 3B top). The effects of the IR illumination disappeared shortly (~50 ms in this example) after the IR pulse ended and the recovery of the exact AP shape is illustrated in Fig. 3B (bottom). The phase plot illustrates the changes in amplitude as well as in the maximum *dv/dt* (Fig. 3C). The averaged reductions in AP amplitude and duration from 7 preparations were 3.4 ± 0.06 mV (mean ± SEM, $p < 0.05$, Paired Student's *t*-test, p is probability value) and 101 ± 2.9 µs (mean ± SEM, $p < 0.05$, Paired Student's *t*-test), respectively. The effect of short IR pulses (20 ms) on muscle activities was also studied

and similar findings recorded. The muscle recording was conducted in a similar manner to the axonal recording, described in Section 2.1, with the current injection electrode and voltage recording electrode positioned close to each other. In Fig. 3E the inhibition of a Ca^{2+} spike due to illumination of a single IR pulse (12.6 mW, 30 ms) is illustrated. However, for this report, the focus will be on the axonal recordings.

3.2 Long IR Pulse Blocks Locally Induced APs

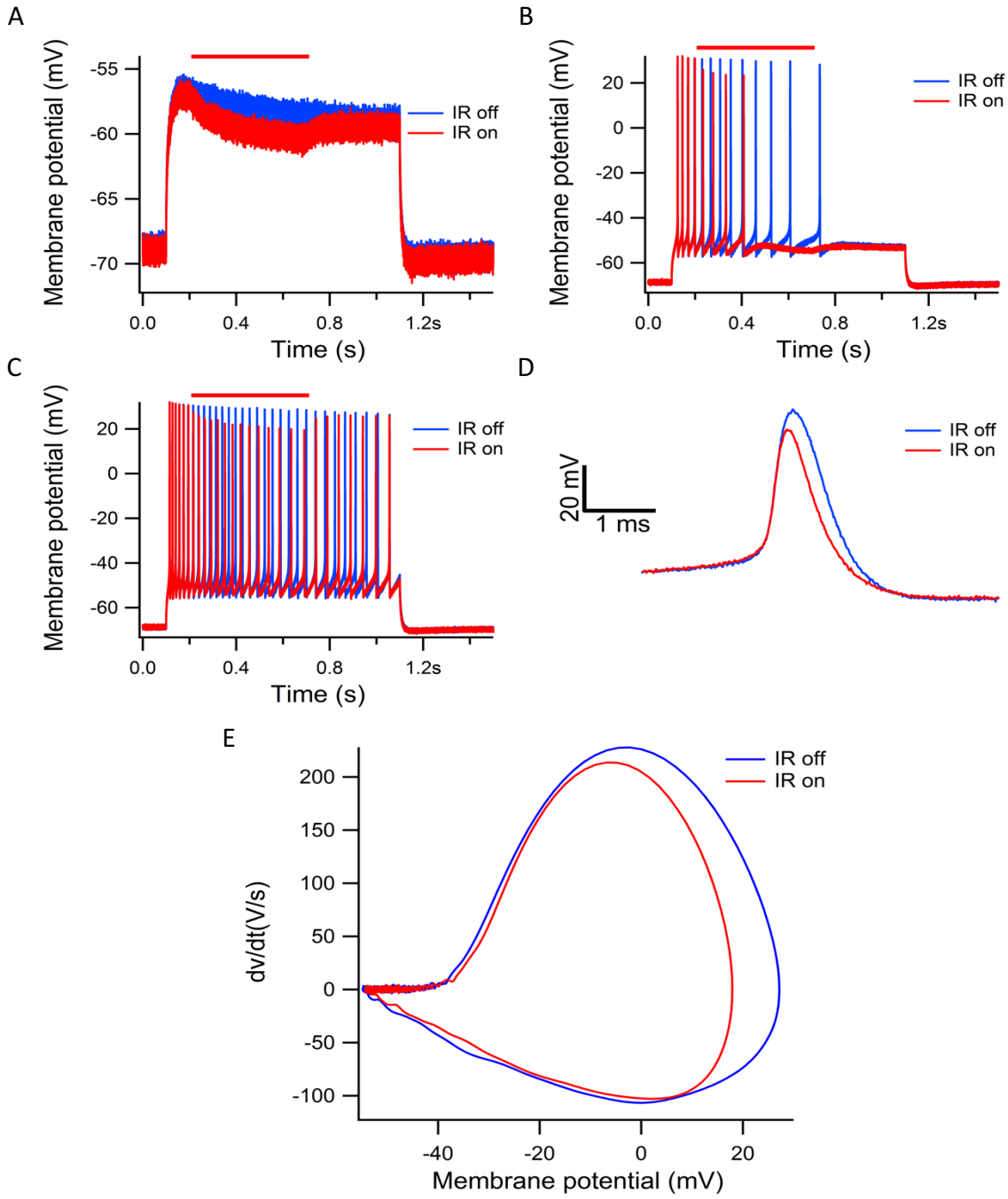

Figure 4: 500 ms IR pulses blocked AP. (A), (B) and (C) IR effects on membrane potential with different current injection steps (10 nA, 15 nA and 22 nA). The red bars above indicate the timing of IR pulses. (D) Comparison of AP waveforms expanded in time scale with and without IR. (E) Phase plot of the two APs in (D).

In addition to the short IR pulses, the effects of significantly longer IR pulses with 500 ms duration on the axonal excitability were also studied. The temperature rise induced by this long IR pulse was 11.8 ± 0.52 ℃ (mean ± SEM, $N = 5$). Figure 4A, B and C illustrate representative traces when the preparation was illuminated by single IR pulse with a power of 7.1 mW and duration of 500 ms. An IR pulse delivered during subthreshold current injection steps (10 nA) slightly reduced the membrane potential (Fig. 4A red) when compared to that without IR pulse (Fig. 4A blue). APs initiated by a current step (15 nA) slightly above AP firing threshold level could be inhibited by the IR pulse (Fig. 4B). An IR pulse delivered during high frequency AP firing (22 nA current injection) caused a progressive decrease in AP amplitude and a slight decrease in firing frequency (Fig. 4C), while the AP threshold and afterhyperpolarization were minimally affected. Complete recovery was observed 400 ms after delivery of the IR pulse. A comparison of the AP waveforms with (Fig. 4D red) and without (Fig. 4D blue) IR pulse illumination shows a significant decrease in amplitude (~ 10 mV) and duration (~ 150 μs). The phase plot of these two APs illustrates the changes in amplitude as well as in *dv/dt* maximum and *dv/dt* minimum (Fig. 4E).

3.3 IR Pulses Reduce Input Resistance

Studies of the impact of the IR illumination on input resistance were performed as well. Figure 5A shows a small reduction in membrane voltage in both hyperpolarizing and subthreshold depolarizing directions, which suggests a decrease in input resistance in comparison to the control trace. For a single IR pulse with an optical power of 7.1 mW and a duration of 500 ms, the average membrane potential change that occurred during the last 20 ms of the applied IR pulse is plotted against the subthreshold current injection steps (Fig. 5B). The membrane potential measured in the absence of an IR pulse was obtained from the same time window as that with IR pulse. Each data point was averaged over 5-10 different trials to obtain representative data. A linear fit illustrates the decrease in input resistance (slope) and a slight shift of reversal potential towards more negative direction. The average decrease in input resistance from five preparations is 8.4 % ± 0.56% (mean ± SEM, $p < 0.05$, Paired Student's *t*-test).

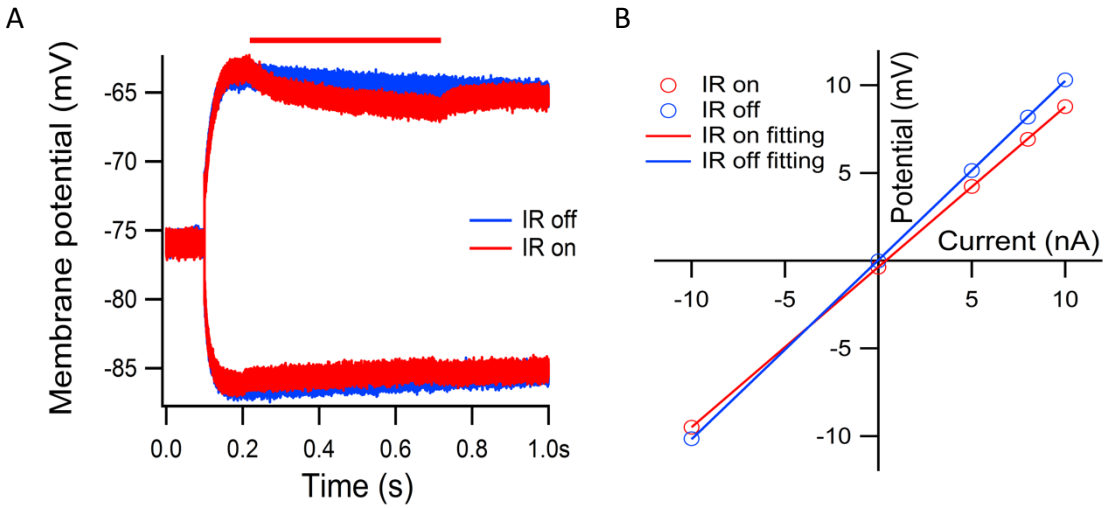

Figure 5: Effect of a 500 ms IR pulse on input resistance. (A) The IR pulse decreases the input resistance and shifts the reversal potential. (B) Linear fit of the average membrane potential change recorded during the last 20 ms of a single 500 ms long IR pulse versus the amplitude of subthreshold current injections. Control data was obtained from the same time windows. Each data point was averaged over 5 – 10 trials.

DISCUSSION

In this report, we used the inhibitory motor axon and muscle fiber of the crayfish opener preparation to investigate the effects of a 2 μm IR laser pulse on neural and muscular excitability. We found that the IR square pulse delivered to a small region of the axon inhibits the generation of the amplitude and duration of the APs. Similar IR inhibition on muscle Ca^{2+} spikes were observed. Modulations on the AP firing frequency and the rates of AP depolarization and repolarization were recorded. Since there is a reduction in input resistance due to the IR pulse, this reduction could contribute to the inhibition

we reported here. However, as the IR light induced local temperature increase is not insignificant (8 – 12 ℃), a temperature dependent change in Na^+ and K^+ channel kinetics could also potentially play an important role in the IR induced inhibition so that further studies are ongoing.

The inhibitory effect we have observed can be due to temperature dependent changes in membrane resistance and channel kinetics. Specifically, previous studies have shown that membrane resistance decreased with increase in temperature[23]. A recent study on Chinese hamster ovarian cells found that the membrane fluidity increased with IR pulse exposure[24]. This parameter alone however may not be sufficient to completely account for the inhibition we observed because of the small decrease (8.4%) in input resistance induced by the IR light. We believe that the predominant mechanisms that underline IR inhibition reported here can possibly be due to effects caused by IR-induced temperature increase on channel kinetics. Previous studies in the frog myelinated axon suggested that raising the temperature can accelerate the activation of Na^+ channels[25]. However, the temperature dependent accelerations of K^+ channel activation and Na^+ inactivation are stronger than that of the Na^+ channel activation. The net result of such a non-uniform temperature sensitivity of channel kinetic parameters is that the contribution of the Na^+ ion flow to the rising phase of the AP can be weakened at higher temperatures. Concomitantly, a fast K^+ channel activation accelerates the AP repolarization. These channel dynamics changes can enforce each other to reduce the AP amplitude and duration.

Here we used an IR wavelength centered close to 2 μm, at which water has a relatively high absorption coefficient, and a smaller optical fiber of 50 μm core diameter than previous IR inhibition reports[13-19]. Single IR pulses of 500 ms long duration were applied to characterize IR inhibition effects on APs and input resistance. IR-induced temperature rises were monitored simultaneously with electrophysiological recordings. Overall, the crayfish opener neuromuscular junction was studied in conjunction with IR inhibition for the first time. With TECC, our results also illustrate a subtler impact of IR modulation on Na^+ and Ca^{2+} spikes and input resistance in the terms of signal processing at the single spike and single cell levels. Modeling will provide a way to quantitatively assess the impact of the local reduction in membrane resistance. Further studies with additional optical performance, temporal and spatial parameter variations will be important to gain further insights into the intricate interplay between the thermal effects, membrane resistance and associated channel dynamics on IR induced neural inhibition.

ACKNOWLEDGEMENTS

We would like to thank Feiyuan Yu for helping with the crayfish preparations. This research is based upon work supported by the Air Force Office of Scientific Research (AFOSR) under grant FA9550-17-1-0276.

REFERENCES

[1] Wells, J., Kao, C., Mariappan, K., Albea, J., Jansen, E. D., Konrad, P., & Mahadevan-Jansen, A., "Optical stimulation of neural tissue in vivo," Optics Letters, 30(5), 504 (2005).
[2] Jenkins, M. W., Duke, A. R., Gu, S., Doughman, Y., Chiel, H. J., Fujioka, H., Watanabe, M., Jansen, E. D., Rollins, A. M., "Optical pacing of the embryonic heart," Nature Photonics, 4(9), 623–626 (2010).
[3] Wells, J., Kao, C., Konrad, P., Milner, T., Kim, J., Mahadevan-Jansen, A., & Jansen, E. D., "Biophysical Mechanisms of Transient Optical Stimulation of Peripheral Nerve," *Biophysical Journal*, *93*(7), 2567–2580 (2007).
[4] Shapiro, M. G., Homma, K., Villarreal, S., Richter, C.-P., & Bezanilla, F., "Infrared light excites cells by changing their electrical capacitance," *Nature Communications*, *3*(1), 736 (2012).
[5] Liu, Q., Frerck, M. J., Holman, H. A., Jorgensen, E. M., & Rabbitt, R. D., "Exciting Cell Membranes with a Blustering Heat Shock," *Biophysical Journal*, *106*(8), 1570–1577 (2014).
[6] Dittami, G. M., Rajguru, S. M., Lasher, R. A., Hitchcock, R. W., & Rabbitt, R. D., "Intracellular calcium transients evoked by pulsed infrared radiation in neonatal cardiomyocytes," *The Journal of Physiology*, *589*(6), 1295–1306 (2011).
[7] Cayce, J. M., Bouchard, M. B., Chernov, M. M., Chen, B. R., Grosberg, L. E., Jansen, E. D., Hillman, E. M.C., Mahadevan-Jansen, A., "Calcium imaging of infrared-stimulated activity in rodent brain," *Cell Calcium*, *55*(4), 183–190 (2014).

[8] Lumbreras, V., Bas, E., Gupta, C., & Rajguru, S. M., "Pulsed infrared radiation excites cultured neonatal spiral and vestibular ganglion neurons by modulating mitochondrial calcium cycling," *Journal of Neurophysiology*, *112*(6), 1246–1255 (2014).
[9] Albert, E. S., Bec, J. M., Desmadryl, G., Chekroud, K., Travo, C., Gaboyard, S., Bardin, F., Marc, I., Dumas, M., Lenaers, G., Hamel, C., Muller, A., Chabbert, C., "TRPV4 channels mediate the infrared laser-evoked response in sensory neurons," Journal of Neurophysiology, *107*(12), 3227–3234 (2012).
[10] Beier, H. T., Tolstykh, G. P., Musick, J. D., Thomas, R. J., & Ibey, B. L., "Plasma membrane nanoporation as a possible mechanism behind infrared excitation of cells," *Journal of Neural Engineering*, *11*(6), 066006 (2014).
[11] Schultz, M., Baumhoff, P., Maier, H., Teudt, I. U., Krüger, A., Lenarz, T., & Kral, A., "Nanosecond laser pulse stimulation of the inner ear-a wavelength study," *Biomedical Optics Express*, *3*(12), 3332–3345 (2012).
[12] Rettenmaier, A., Lenarz, T., & Reuter, G., "Nanosecond laser pulse stimulation of spiral ganglion neurons and model cells," *Biomedical Optics Express*, *5*(4), 1014 (2014).
[13] Cayce, J. M., Friedman, R. M., Jansen, E. D., Mahavaden-Jansen, A., & Roe, A. W., "Pulsed infrared light alters neural activity in rat somatosensory cortex in vivo," *NeuroImage*, *57*(1), 155–166 (2011).
[14] Duke, A. R., Jenkins, M. W., Lu, H., McManus, J. M., Chiel, H. J., & Jansen, E. D., "Transient and selective suppression of neural activity with infrared light," *Scientific Reports*, *3*(1), 2600 (2013).
[15] Lothet, E. H., Kilgore, K. L., Bhadra, N., Bhadra, N., Vrabec, T., Wang, Y. T., Jansen, E. D., Jenkins, M. W., Chiel, H. J., "Alternating current and infrared produce an onset-free reversible nerve block," Neurophotonics, 1(1), 011010 (2014).
[16] Walsh, A. J., Tolstykh, G. P., Martens, S., Ibey, B. L., & Beier, H. T., "Action potential block in neurons by infrared light," *Neurophotonics*, *3*(4), 040501 (2016).
[17] Duke, A. R., Lu, H., Jenkins, M. W., Chiel, H. J., & Jansen, E. D., "Spatial and temporal variability in response to hybrid electro-optical stimulation," *Journal of Neural Engineering*, *9*(3), 036003 (2012).
[18] Lothet, E. H., Shaw, K. M., Lu, H., Zhuo, J., Wang, Y. T., Gu, S., Stolz, D. B., Jansen, E. D., Horn, C. C., Chiel, H. J., Jenkins, M. W., "Selective inhibition of small-diameter axons using infrared light," Scientific Reports, 7(1), 3275 (2017).
[19] Wang, Y. T., Rollins, A. M., & Jenkins, M. W., "Infrared inhibition of embryonic hearts," *Journal of Biomedical Optics*, *21*(6), 60505 (2016).
[20] Huxley, A. F., "ION MOVEMENTS DURING NERVE ACTIVITY," *Annals of the New York Academy of Sciences*, *81*(2), 221–246 (1959).
[21] Hodgkin, A. L., & Katz, B., "The effect of temperature on the electrical activity of the giant axon of the squid," *The Journal of Physiology*, *109*(1–2), 240–249 (1949).
[22] Yao, J., Liu, B., and Qin, F, "Rapid Temperature Jump by Infrared Diode Laser Irradiation for Patch-Clamp Studies," *Biophysical Journal 96*(9), 3611–3619 (2009).
[23] Payton, B. W., Bennett, M. V. L., Pappas, G. D., "Temperature-dependence of resistance at an electrotonic synapse," *Science*, 165(3893), 594–597 (1969).
[24] Walsh AJ, Cantu JC, Ibey BL, Beier HT, "Short infrared laser pulses increase cell membrane fluidity," Proc. SPIE 10062, 100620D (2017).
[25] Frankenhaeuser B, Moore LE, "The effect of temperature on the sodium and potassium permeability changes in myelinated nerve fibres of *Xenopus laevis*," *J Physiol*., 169(2), 431-437 (1963).